Progress In Electromagnetics Research, Vol. 134, 337–357, 2013

THEORY OF ZERO-POWER RFID SENSORS BASED ON HARMONIC GENERATION AND ORTHOGONALLY POLARIZED ANTENNAS

Federico Alimenti* **and Luca Roselli**

Department of Electronic and Information Engineering, University of Perugia, Italy

Abstract—In this paper a novel approach is proposed to solve the issue of the absolute accuracy required by the most of the passive chip-less RFID sensors. To this purpose the sensor information is encoded as the phase difference between two signals, one of the two acting as the reference signal for the other one. First the tag receives a carrier at frequency f_0, then two equal signals at frequency $2f_0$ are generated by means of a diode-based frequency doubler and a power divider. At this point one of the two signals is phase-shifted using a passive sensing element. Finally the $2f_0$ signals are re-irradiated by exploiting two orthogonally polarized antennas. With this approach the sensor information can be extracted by a suitable reader equipped with two complex (I/Q) receivers. The idea will be first developed from a theoretical basis and then verified with several particular cases. The novel tag concept is compatible with paper substrate and inkjet printing technology since antennas diodes and passive sensing elements, i.e., all the main tag components, are going to be developed on paper materials.

1. INTRODUCTION

The short-range wireless transmission of sensor information finds application is several fields ranging from the monitoring of biological parameters in medicine [1–6], to the measurements of mechanical quantities in industrial applications [7–10] and robot guidance [11]. In the last years several technologies have been developed to this purpose, but the emerging one is based on the Radio-Frequency IDentification (RFID) concept [12], due to the convergence of several new ideas

Received 1 September 2012, Accepted 29 October 2012, Scheduled 1 December 2012
* Corresponding author: Federico Alimenti (alimenti@diei.unipg.it).

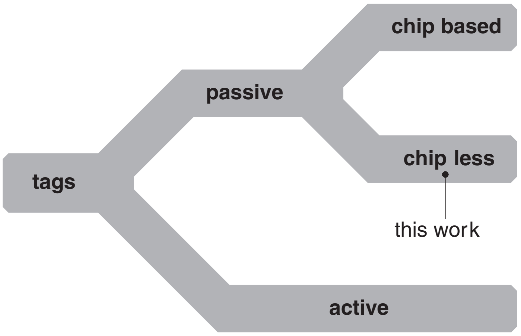

Figure 1. Classification of the RFID tag technologies.

and approaches such as the RF-energy harvesting [13, 14], RF-carrier reuse, load modulation method, organic [15–21] and inkjet printed [22–27] electronics. The RF energy harvesting and RF-carrier reuse, for example, allow for battery-less (i.e., passive) RFID sensors that can operate for years without any maintenance.

A classification of the available tag technologies is sketched in Fig. 1. The passive systems can be divided in two families, namely: chip-based and chip-less tags. The first family exploits usually a low-power CMOS chip to implement the main tag functions (RF carrier rectification, DC voltage regulation, ASK demodulation, ID decoding, load modulation, etc.) and thus can be adapted to sensor applications by a few additional circuit blocks (signal conditioning, ADC, etc.). The main advantage of such an approach is the digital modulation of the transmitted signal, and thus the reliability of the data treatment, as shown in [28, 29]. The production costs of chip based tags are mostly associated to the heterogeneous integration of the silicon chip with the antenna [30, 31], the latter being typically fabricated on a flexible substrate or textile substrate [32–37].

In order to reduce the above mentioned costs, the chip-less tag family has been introduced and applied to wireless sensing in last years [38–43]. The chip-less RFID sensor tags exploit an antenna, the electrical properties of which are controlled by the change of the physical parameter to be measured. There are, mostly, two proposed approaches: the first is to induce a permanent change in the antenna property when a certain critical threshold (acceleration, temperature, fluid level, etc.) is exceeded [10]. The second exploits a sensing load, the impedance of which is controlled by the sensed variable, connected to an antenna [44]. In both cases the wireless sensor system (tag and reader) needs to have an absolute accuracy, this limiting the system performance with respect to both distance and fabrication tolerances.

A different method has been recently introduced by [45]. In this paper a novel sensing principle is associated to the generation of an inter-modulation signal from a tag, the latter being illuminated by two waves at different frequencies. The advantage of this idea is that the tag response is generated at a perfectly known frequency, thus the presence or the absence of such a signal can hardly be equivocated. Similar techniques have been used in harmonic radar systems [46] and in one-bit frequency doubling tags [47].

In this work a novel and original approach is proposed to solve the issue of absolute accuracy of most passive chip-less RFID sensors. To this purpose the sensor information is encoded as the phase difference between two signals, acting as the reference signal one to each other. First the tag receives a carrier at frequency f_0. Then two equal signals at frequency $2f_0$ are generated by means of a diode-based frequency doubler and a power divider. At this point one of the two signals is phase-shifted using a passive sensing element. Finally the $2f_0$ signals are re-irradiated by exploiting two orthogonally polarized antennas. With this approach the sensor information can be extracted by a suitable reader equipped with two complex (I/Q) receivers. The above tag concept is compatible with paper substrate and inkjet printing technology since antennas [48], diodes [49] and passive sensing elements or [50–53], i.e., all the main tag components, will be soon available on paper material. In addition, Substrate Integrated Waveguide (SIW) structures [54], a way to implement standard waveguide geometries [55] exploiting planar processes and dielectric substrates, will be soon available on paper. As a consequence, a further cost reduction of standard PCB technologies [56] could be directly achieved.

This article is organized as follows. The sensor architecture is described in Section 2 where both tag and reader sub-systems are considered. Then, Section 3 illustrates the theory of operation and the basic equations needed to recover the information. Finally the developed theory is verified in Section 4 by means of four particular cases.

2. SENSOR ARCHITECTURE

The proposed RFID sensor is based on the harmonic radar concept [57, 58], i.e., on tag that, being illuminated by a carrier at frequency f_0, is capable of generating the second harmonic $2f_0$. Such a tag, however, is also responsible for the sensor information encoding, as shown in Fig. 2.

To describe the tag operation let's consider the signal flow shown

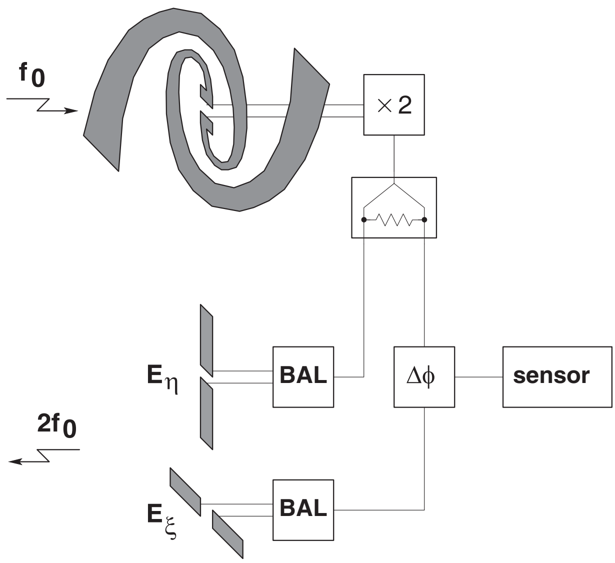

Figure 2. Harmonic tag block diagram.

in the same figure. The incoming electromagnetic wave at frequency f_0 is received by a spiral or an helical antenna [59]. In this way the power at the antenna output is maximized regardless of the polarization or the relative reader-tag orientation. The received power is then fed into a varactor or a Schottky diode frequency doubler [60] and the second harmonic is generated. At this point the $2f_0$ signal is split by a power divider. The first part is directly re-irradiated in vertical polarization (e.g., E_η in Fig. 2) in such a way as to form a reference signal component. The second part, instead, is phase-shifted by the angle Δ_φ and then re-irradiated in horizontal polarization (e.g., E_ξ in Fig. 2). Phase shifters based on the concept proposed in [61] could, for example, be used to this purpose.

The phase angle Δ_φ encodes the sensor information and must be recovered by the reader. To this purpose the reader is composed of four sub-systems, as depicted in Fig. 3. A Phase Locked Loop (PLL) oscillator is used to generate both the f_0 and the $2f_0$ signals in a synchronous way.

The f_0 carrier is managed by the transmitter (TX) and serves to remotely illuminate the tag. The transmitter operates in Continuous Wave (CW) mode or exploiting a modulated carrier (see M input in Fig. 3). It is composed by a modulator and a power amplifier, the latter followed by a band-pass filter at f_0 (or a stop-band filter a

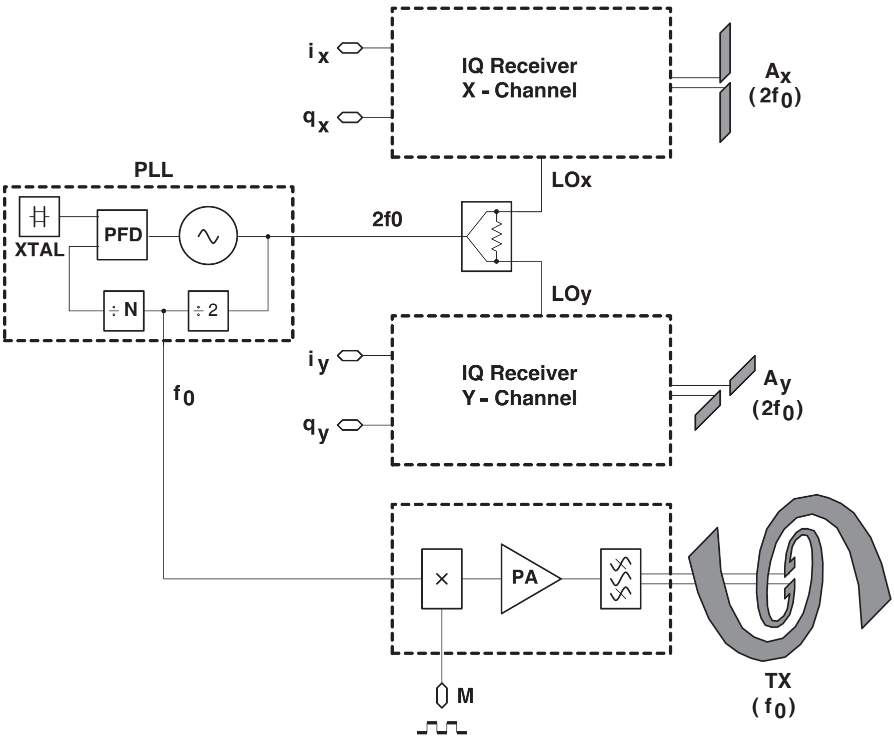

Figure 3. Reader block diagram.

$2f_0$). The filter is necessary to significantly reduce the second-harmonic generated by the power amplifier, thus eliminating the risk of blinding the receiver. The second harmonic of the TX, in-fact, should be kept below the noise floor of the receiver.

The transmitting antenna is again of spiral or helical type in order to maximize the illumination power regardless of the orientation.

The $2f_0$ component, instead, is used as the local oscillator of the receiver. Such a signal is thus divided in two parts and applied to both the x- and y-receiver channels. Each channel is sensitive to a particular wave polarization, this by exploiting dipole antennas. In particular, the x-channel is adopted to receive the vertical polarization signal while, the y-channel is exploited for the horizontally polarized one. Because the sensor information is encoded as phase difference Δ_φ between the two polarizations, a vector receiver is needed for each channel. This vector receiver is based on a zero-IF In-phase and Quadrature (IQ) architecture, as illustrated in Fig. 4.

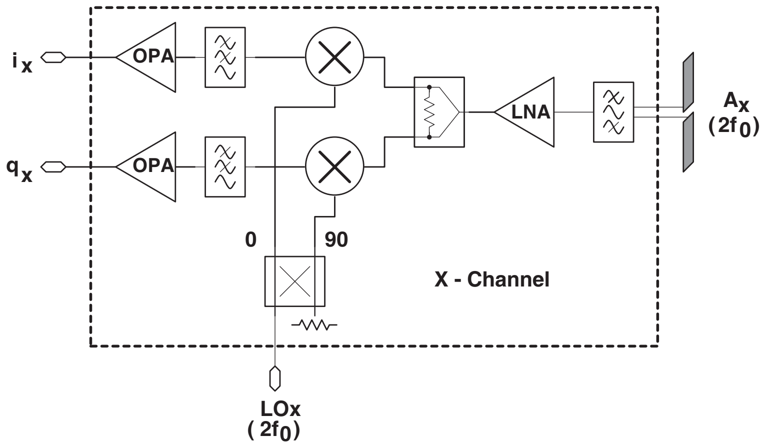

Figure 4. IQ receiver (x-channel) block diagram.

3. THEORY

This section is devoted to the operation theory of the novel RFID sensor system. First, the detection of the two orthogonal $2f_0$ plane waves is considered. These waves are generated and irradiated by the tag whereas the relevant phase and amplitude information associated to them is recovered by the reader. The illumination of the tag with a carrier at f_0, the second harmonic generation and the phase information coding will be also treated in this section.

The theory will be developed under the basic assumption to have a tag antenna plane parallel to the reader antenna plane. In addition the two antenna systems will be considered axially aligned along the propagation direction. This hypothesis is satisfied in many industrial applications such as the contact-less measurement of mechanical quantities in rotating systems like engines and turbines [62] or monitoring of objects above a conveyor belt in a distribution chain. In the last case the tag is assumed to be interrogated when it is exactly perpendicular to the reader.

3.1. Tag Information Encoding

The proposed RFID sensor relies on the phase and amplitude information written on two orthogonally polarized plane waves at frequency $2f_0$. These waves are fully determined by the knowledge of the associated electric field vectors as in Fig. 5. In particular, the ξ-η coordinate system is used in the tag plane while the two electric fields

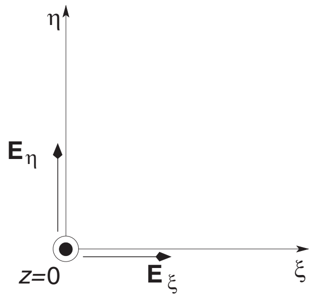

Figure 5. Coordinate system adopted in the tag plane (i.e., ξ-η plane) and $2f_0$ electric field components. These electric fields are irradiated by the two equal orthogonal tag antennas.

$\mathbf{E}_\xi$ and $\mathbf{E}_\eta$ are irradiated by two equal antennas, linearly polarized along ξ and η respectively.

Adopting the complex vector formalism one can write:

$$\begin{aligned} \mathbf{E}_\xi &= E_\xi e^{j\varphi_\xi}\mathbf{u}_\xi \\ \mathbf{E}_\eta &= E_\eta e^{j\varphi_\eta}\mathbf{u}_\eta \end{aligned} \tag{1}$$

where E_k, φ_k and $\mathbf{u}_k$, with $k = \xi$, η, are the electric filed amplitudes, the electric field phases and the unit vectors respectively. In particular the amplitudes E_k will be assumed real and positive having concentrated all the phase relationships between the two fields in the φ_k values.

As a consequence of (1) the total electric field $\mathbf{E}_T$, irradiated by the tag at $2f_0$, is given by:

$$\begin{aligned} \mathbf{E}_T &= \mathbf{E}_\xi + \mathbf{E}_\eta \\ &= E_\xi e^{j\varphi_\xi}\left[\mathbf{u}_\xi + \frac{E_\eta}{E_\xi}e^{j\Delta\varphi}\mathbf{u}_\eta\right] \end{aligned} \tag{2}$$

with $E_\xi \neq 0$ and $\Delta\varphi$ being the phase difference between the two fields:

$$\Delta\varphi = \varphi_\eta - \varphi_\xi \tag{3}$$

It is worth noticing that (2) is the general expression for an elliptical polarized plane wave. As particular cases both purely linear ($\Delta\varphi = 0, \pi$) and purely circular ($E_\eta/E_\xi = 1$ and $\Delta\varphi = \pm\pi/2$) polarizations are allowed. This means that the relevant tag information can be encoded either in the phase difference $\Delta\varphi$ or in the amplitude ratio E_η/E_ξ.

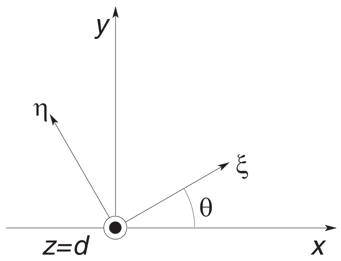

Figure 6. Coordinate system adopted in the reader plane (i.e., x-y plane). The reader plane is parallel to the tag plane. The tag ξ-η coordinate system is rotated by an angle ϑ with respect to the reader x-y coordinate system. The distance between reader and tag is equal to d.

3.2. Received Reader Voltages

Let's now consider a reader placed at a distance d from the tag. The reader exploits two equal linear polarized antennas in orthogonal directions to detect the elliptical polarized wave generated by the tag. This situation is summarized in Fig. 6, where the reader antenna plane has been assumed parallel to the tag antenna plane. In this scheme the two reader antennas are placed along the x- and the y-axis. Moreover, an angle ϑ is formed between ξ- and x-axis. Such an angle will, in general, not known since it depends on the way the tag is attached to the object to be monitored.

As a final assumption let us consider the case when the reader and the tag antenna systems are perfectly aligned along a common z-axis. In this case the electric field at the reader location $\mathbf{E}_R$ is simply given by the tag field $\mathbf{E}_T$ multiplied for the transfer function of the channel:

$$\mathbf{E}_R = \alpha e^{-j\beta d} \mathbf{E}_T \tag{4}$$

where α is the path loss, β is the propagation constant and d is the reader-tag distance. If a free-space radiation model can be applied to the considered problem, α and β are:

$$\begin{aligned} \alpha &= \frac{\lambda}{4\pi d}\sqrt{D_R D_T} \\ \beta &= \frac{2\pi}{\lambda} \end{aligned}$$

In (5) the wavelength λ is evaluated at $2f_0$, whereas D_R and D_T are the reader and the tag antenna directivity, respectively. The electric field at the reader location $\mathbf{E}_R$ can then be projected along the x-oriented receiver antenna:

$$\begin{aligned} E_x &= \mathbf{E}_R \cdot \mathbf{u}_x \\ &= E_0 \left[\mathbf{u}_\xi \cdot \mathbf{u}_x + \frac{E_\eta}{E_\xi} e^{j\Delta\varphi} \mathbf{u}_\eta \cdot \mathbf{u}_x \right] \end{aligned} \tag{5}$$

similarly, for the y-oriented receiver antenna one gets:

$$\begin{aligned} E_y &= \mathbf{E}_R \cdot \mathbf{u}_y \\ &= E_0 \left[\mathbf{u}_\xi \cdot \mathbf{u}_y + \frac{E_\eta}{E_\xi} e^{j\Delta\varphi} \mathbf{u}_\eta \cdot \mathbf{u}_y \right] \end{aligned} \tag{6}$$

In (5) and (6) the phasor E_0 is defined as:

$$E_0 = \alpha e^{j\left(\varphi_\xi - \beta d\right)} E_\xi \tag{7}$$

Considering that the projections of the ξ and η unity vectors along the x and y directions are given by:

$$\begin{aligned} \mathbf{u}_\xi \cdot \mathbf{u}_x &= \cos\vartheta \\ \mathbf{u}_\eta \cdot \mathbf{u}_x &= -\sin\vartheta \\ \mathbf{u}_\xi \cdot \mathbf{u}_y &= \sin\vartheta \\ \mathbf{u}_\eta \cdot \mathbf{u}_y &= \cos\vartheta \end{aligned} \tag{8}$$

one obtains:

$$E_x = E_0 \left[\cos\vartheta - \frac{E_\eta}{E_\xi} e^{j\Delta\varphi} \sin\vartheta \right] \tag{9}$$

$$E_y = E_0 \left[\sin\vartheta + \frac{E_\eta}{E_\xi} e^{j\Delta\varphi} \cos\vartheta \right] \tag{10}$$

The E_x and E_y fields can be finally related to the received voltages processed by the two reader's channels. To this purpose one can exploit the effective antenna length l_e as defined in [63, p. 305]. The input received voltages are:

$$V_k^i = l_e E_k \tag{11}$$

where $k = x, y$ and the apex i stands for input. If, for example, an half-wave dipole antenna is considered, the maximum l_e is:

$$l_e = \frac{\lambda}{\pi} \tag{12}$$

which is smaller than $\lambda/2$ due to the sinusoidal distribution of the current along the dipole itself. Inserting (9) and (10) in (11) and using the Euler's formula to express $e^{j\Delta\varphi}$ one gets:

$$V_x^i = l_e E_0 \left(A_x + jB_x \right) \tag{13}$$

$$V_y^i = l_e E_0 \left(A_y + jB_y\right) \tag{14}$$

where the A and B quantities contain all the relevant tag information, i.e., $\Delta\varphi$, E_η/E_ξ and ϑ:

$$\begin{aligned} A_x &= \cos\vartheta - \frac{E_\eta}{E_\xi}\cos\Delta\varphi\sin\vartheta \\ A_y &= \sin\vartheta + \frac{E_\eta}{E_\xi}\cos\Delta\varphi\cos\vartheta \end{aligned} \tag{15}$$

$$\begin{aligned} B_x &= -\frac{E_\eta}{E_\xi}\sin\Delta\varphi\sin\vartheta \\ B_y &= \frac{E_\eta}{E_\xi}\sin\Delta\varphi\cos\vartheta \end{aligned} \tag{16}$$

The time-domain signals are easily obtained from the phasors in (13), (14) and considering the expression of E_0 quoted in (7). The x-channel input voltage is given by:

$$\begin{aligned} v_x^i(t) &= \Re\left\{V_x^i e^{j2\omega_0 t}\right\} = V_0 \Re\left\{\left(A_x + jB_x\right) e^{j\left(2\omega_0 t + \varphi_\xi - \beta d\right)}\right\} \\ &= V_0\left[A_x \cos\left(2\omega_0 t + \varphi_\xi - \beta d\right) - B_x \sin\left(2\omega_0 t + \varphi_\xi - \beta d\right)\right] \end{aligned} \tag{17}$$

V_0 being the amplitude of the input referred voltage:

$$V_0 = l_e\left|E_0\right| = \alpha l_e E_\xi \tag{18}$$

Similarly, y-channel input voltage can be written as:

$$v_y^i(t) = V_0\left[A_y \cos\left(2\omega_0 t + \varphi_\xi - \beta d\right) - B_y \sin\left(2\omega_0 t + \varphi_\xi - \beta d\right)\right] \tag{19}$$

3.3. Conversion Products

Once the time-domain expression have been obtained, it is quite straightforward to derive the conversion products and, from them, the in-phase $i(t)$ and quadrature $q(t)$ output signal components. For the x-channel one obtains:

$$i_x(t) = \text{LPF}\left\{2G_v^{rx} v_x^i(t)\cos(2\omega_0 t - \psi)\right\} = G_v^{rx} V_0 (A_x \cos\psi_R - B_x \sin\psi_R) \tag{20}$$

$$q_x(t) = \text{LPF}\left\{-2G_v^{rx} v_x^i(t)\sin(2\omega_0 t - \psi)\right\} = G_v^{rx} V_0 (A_x \sin\psi_R + B_x \cos\psi_R) \tag{21}$$

where G_v^{rx} is the overall receiver gain, ψ is the local oscillator phase and LPF $\{\}$ is the low-pass operator cutting the $4\,\omega_0$ mixing product. The quantity ψ_R is defined as:

$$\psi_R = \psi + \varphi_\xi - \beta d \tag{22}$$

Similarly, the y-channel outputs are:

$$i_y(t) = G_v^{rx} V_0\left(A_y \cos\psi_R - B_y \sin\psi_R\right) \tag{23}$$

$$q_y(t) = G_v^{rx} V_0 \left(A_y \sin\psi_R + B_y \cos\psi_R\right) \tag{24}$$

In the case of a modulated carrier (signal injected at the M input in Fig. 3), (20)–(24) represent the amplitude of the base-band signal at the receiver output. As a final observation it is worth noticing that the same receiver gain G_v^{rx} and local oscillator phase ψ have been assumed for both the x and the y reader's channels. In practice this condition can be met by calibrating the two receivers with a set of preliminary measurements.

3.4. Information Recovery

The relationships (20), (21) and (23), (24) constitute a set of 4 equations that can be written at each time instant. The known terms are given by the in-phase and quadrature signals at the output of the two reader's channels, i.e., by measurable values. The unknowns are the received amplitude V_0, the overall received phase ψ_R and the tag quantities, namely: ϑ, $\Delta\varphi$ and E_η/E_ξ. As a results 5 unknowns are obtained, this means that additional knowledge of the system is needed. For example, if the tag is designed to have a determined E_η/E_ξ ratio, all the information is encoded within $\Delta\varphi$.

In order to eliminate V_0 and ψ_R from the above system of equations the following ratio is computed at each time instant:

$$U = U_R + jU_I = \frac{i_x + jq_x}{i_y + jq_y} \tag{25}$$

Developing the above expression one obtains:

$$U_R = \frac{i_x i_y + q_x q_y}{i_y^2 + q_y^2} = \frac{A_x A_y + B_x B_y}{A_y^2 + B_y^2} \tag{26}$$

$$U_I = \frac{q_x i_y - i_x q_y}{i_y^2 + q_y^2} = \frac{B_x A_y - A_x B_y}{A_y^2 + B_y^2} \tag{27}$$

The U_R and U_I values can be directly evaluated from the measured output voltages (known terms), whereas the tag unknowns are within the A and B quantities. The relationship between U_R, U_I and these unknowns can be found by inserting Equations (15), (16) in (26), (27). After some manipulation one obtains:

$$U_R = \frac{1}{D_u}\left\{\left[1 - \left(\frac{E_\eta}{E_\xi}\right)^2\right]\cos\vartheta\sin\vartheta + \frac{E_\eta}{E_\xi}\cos\Delta\varphi\left(\cos^2\vartheta - \sin^2\vartheta\right)\right\} \tag{28}$$

$$U_I = -\frac{1}{D_u}\frac{E_\eta}{E_\xi}\sin\Delta\varphi \tag{29}$$

where the denominator D_u is given by:

$$D_u = \sin^2\vartheta + \left(\frac{E_\eta}{E_\xi}\right)^2 \cos^2\vartheta + 2\frac{E_\eta}{E_\xi}\cos\vartheta\sin\vartheta\cos\Delta\varphi \tag{30}$$

4. RESULTS

The results of the above general theory will now be analyzed in a number of particular cases of practical interest. The first case is that of a tag with fixed (and a-priori known) orientation angle θ, in which the information is encoded by the amplitude only. This assumption means that $\Delta\varphi$ is constant, whereas $\rho = E_\eta/E_\xi$ is varied according to the physical quantity to be measured. If $\theta = 0$ and $\Delta\varphi = 0$, Equations (26), (27) reduce to:

$$U_R = \frac{E_\xi}{E_\eta} \tag{31}$$

$$U_I = 0 \tag{32}$$

As a consequence the information can immediately be derived by U_R, thus identifying a very simple method of zero-power wireless transmission of sensor data.

In the second case the tag has again a fixed orientation angle $\theta = 0$, but the information is encoded as a variation of the phase angle $\Delta\varphi$ only. Here a unit amplitude ratio between the two tag channels is assumed: $\rho = E_\eta/E_\xi = 1$. As a result Equations (26), (27) reduce to:

$$U_R = \cos\Delta\varphi \tag{33}$$

$$U_I = -\sin\Delta\varphi \tag{34}$$

Again the information can immediately be recovered from U_R and U_I. Note that a digital information could be transmitted by simply switching $\Delta\varphi$ between 0 ($U_R = 1$, $U_I = 0$) and $-\pi/2$ ($U_R = 0$, $U_I = 1$).

Let now consider a situation where θ is not a-priori known and, possibly, variable with time. As discussed above, one can decide to encode the sensor information either in the amplitude ratio $\rho = E_\eta/E_\xi$ or in the phase difference $\Delta\varphi$ of the tag. The third case refers to the amplitude encoding mechanism. To this purpose $\Delta\varphi \neq 0$ because two quantities (i.e., ρ and θ) should now be extracted from the two measured quantities (i.e., U_R and U_I). Thus, in the third application case, $\Delta\varphi = -\pi/2$ is considered. As a results one obtains:

$$U_R = \frac{(1-\rho^2)\sin(2\theta)}{(1+\rho^2)-(1-\rho^2)\cos(2\theta)} \tag{35}$$

$$U_I = \frac{2\rho}{(1+\rho^2)-(1-\rho^2)\cos(2\theta)} \tag{36}$$

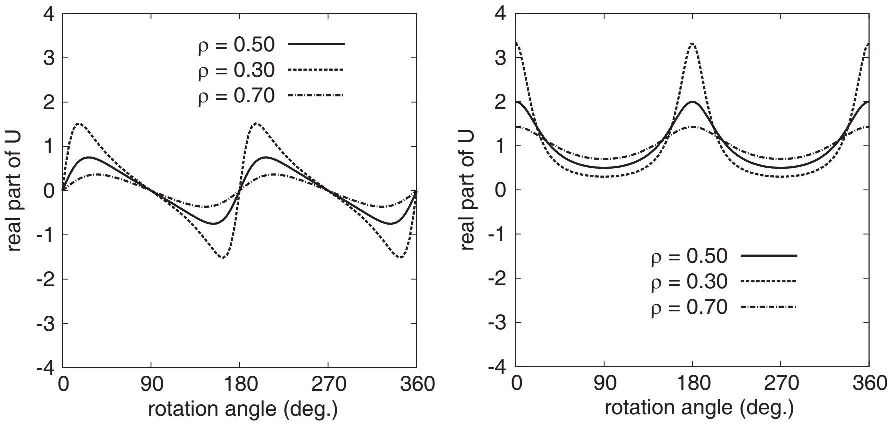

(a) (b)

Figure 7. Real U_R and imaginary U_I parts of the U function versus the rotation angle θ. The function is drawn in the particular case $\Delta\varphi = -\pi/2$ and for three values of $\rho = E_\eta/E_\xi$. Such a parameter has been assumed in the range between 0.3 to 0.7 degrees to avoid singularities when ρ approaches zero.

The previous equations are reported in Fig. 7 as a function of the rotation angle θ and for ρ equal to 0.3, 0.5 and 0.7. At this point it is interesting to note that the proposed reader-tag system can be also used as a wireless rotation sensor. In such a situation the only information is the angle θ, so it is sufficient to set ρ at a fixed value, for example $\rho = 0.5$.

Finally, in the fourth application case, the information is encoded in the phase difference $\Delta\varphi$, whereas it is extracted from the measured quantities along with the orientation angle θ. If $\rho = E_\eta/E_\xi = 1$, Equations (26), (27) becomes:

$$U_R = \frac{\cos\Delta\varphi\cos(2\theta)}{1+\cos\Delta\varphi\sin(2\theta)} \tag{37}$$

$$U_I = \frac{-\sin\Delta\varphi}{1+\cos\Delta\varphi\sin(2\theta)} \tag{38}$$

The function U_R is singular whenever its denominator is equal to zero. This occurs for particular values of the phase $\Delta\varphi$ (i.e., of the phase encoding the sensor information) and of the rotation angle θ. The critical angles can easily be computed and are reported in Table 1. The function U_I, instead, is never singular since, for $\Delta\varphi = n\pi$ with n integer, its numerator is always zero. Nevertheless, for $\Delta\varphi$ close to the critical angles of Table 1, also the U_I values can be very high.

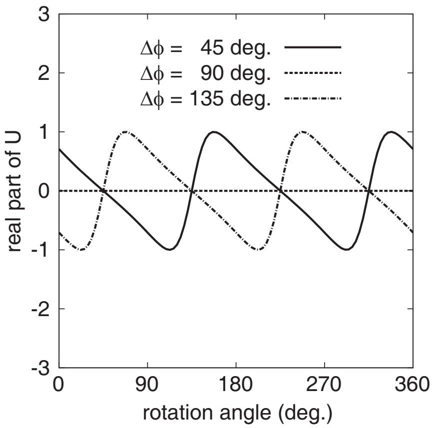

(a)

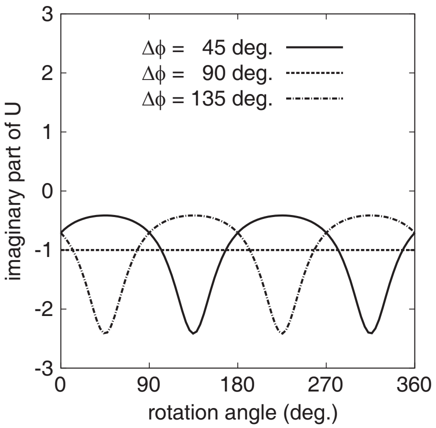

(b)

Figure 8. Real U_R and imaginary U_I parts of the U function versus the rotation angle θ. The function is drawn in the particular case $\rho = E_\eta/E_\xi = 1$ and for three values of $\Delta\,\varphi$. Such a parameter has been assumed in the range between 45 to 135 degrees to avoid singularities.

Table 1. Critical angles.

$\Delta\,\varphi$	θ
$0,\ 2\pi\ \ldots$	$\frac{3}{4}\pi,\ \frac{7}{4}\pi\ \ldots$
$\pi,\ 3\pi\ \ldots$	$\frac{1}{4}\pi,\ \frac{5}{4}\pi\ \ldots$

The singularity problem occurs for those values of $\Delta\varphi$ producing a purely linear wave polarization. Such a problem can always be solved in the following way. When a high value of U_R is detected, the ratio between $(i_y + jq_y)$ and $(i_x + jq_x)$ is evaluated instead of (25). Alternatively, the critical values of $\Delta\varphi$ can be avoided, by conditioning the modulating signal. The latter approach is illustrated in Fig. 8, where U_R and U_I are drawn versus the rotation angle θ and for $\Delta\varphi$ in the 45 to 135 degrees range. It is interesting to note that $\Delta\varphi = \pi/2$ implies a purely circular polarization and thus both U_R and U_I are independent on the rotation angle.

5. CONCLUSIONS

In this work a novel zero-power wireless sensor has been conceived. The sensor is based on harmonic generation and orthogonally polarized waves. The information is encoded in the phase difference or in the amplitude imbalance between two signals that are transmitted in orthogonal polarization. The mathematical development shows that the rotation angle between the sensor and the reader can also be retrieved on the basis of measurable data. Although the developed theory is absolutely general, practical applications could be well targeted in the UHF frequency range ($f_0 = 960\,\mathrm{MHz}$ and $2f_0 = 1920\,\mathrm{MHz}$) or in the WLAN band ($f_0 = 2.45\,\mathrm{GHz}$ and $2f_0 = 4.90\,\mathrm{GHz}$). These results demonstrate the feasibility of the proposed zero-power chip-less sensor tag and of the corresponding reader electronics.

ACKNOWLEDGMENT

The authors wish to acknowledge the University of Perugia for supporting the patent of the system described in this paper. The invention has been filed to the Italian patent office on May 2th, 2012, file number: RM2012A000190.

REFERENCES

1. Sauer, C., M. Stanacevic, G. Cauwenberghs, and N. Thakor, "Power harvesting and telemetry in CMOS for implanted devices," *IEEE Trans. on Circuits and Systems I*, Vol. 52, No. 12, 2605–2613, Dec. 2005.
2. Opasjumruskit, K., T. Thanthipwan, O. Sathusen, P. Sirinamarattana, P. Gadmanee, E. Pootarapan, N. Wongkomet, A. Thanachayanont, and M. Thamsirianunt, "Self-powered wireless temperature sensors exploit RFID technology," *IEEE Pervasive Computing*, Vol. 5, No. 1, 54–61, Jan. 2006.
3. Lu, H. M., C. Goldsmith, L. Cauller, and J.-B. Lee, "MEMS-based inductively coupled RFID transponders for implantable wireless sensor applications," *IEEE Trans. on Magnetics*, Vol. 43, No. 6, 2412–2414, Jun. 2007.
4. Occhiuzzi, C. and G. Marrocco, "The RFID technology for neurosciences: Feasibility of limbs' monitoring in sleep diseases," *IEEE Trans. on Information Technology in Biomedicine*, Vol. 14, No. 1, 37–43, Jan. 2010.
5. Vaz, A., A. Ubarretxena, I. Zalbide, D. Pardo, H. Solar,

A. Garcia-Alonso, and R. Berenguer, "Full passive UHF tag with a temperature sensor suitable for human body temperature monitoring," *IEEE Trans. on Circuits and Systems II: Express Briefs*, Vol. 57, No. 2, 95–99, Feb. 2010.

6. Munnangi, S. R., G. Haobijam, M. Kothamasu, R. Paily, and R. S. Kshetrimayum, "CMOS capacitive pressure sensor design and integration with RFID tag for biomedical applications," *TENCON 2008*, 1–6, Hyderabad, Nov. 2008.
7. Todd, B., M. Phillips, S. Schultz, A. Hawkins, and B. Jensen, "Low-cost RFID threshold shock sensors," *IEEE Sensor Journal*, Vol. 9, No. 4, 464–469, Apr. 2009.
8. Todd, B., M. Phillips, S. Schultz, A. Hawkins, and B. Jensen, "RFID threshold accelerometer," *IEEE Instrumentation and Measurement Magazine*, Vol. 12, No. 4, 14–18, Apr. 2009.
9. Sample, A., D. Yeager, P. Powledge, A. Mamishev, and J. Smith, "Design of an RFID-based battery-free programmable sensing platform," *IEEE Trans. on Instrumentation and Measurement*, Vol. 57, No. 11, 2608–2615, Nov. 2008.
10. Bhattacharyya, R., C. Floerkemeier, and S. Sarma, "Low-cost, ubiquitous RFID-tag-antenna-based sensing," *Proceedings of the IEEE*, Vol. 98, No. 9, 1593–1600, Sep. 2010.
11. M. Kim, K. Kim, and N. Chong, "RFID based collision-free robot docking in cluttered environment," *Progress In Electromagnetics Research*, Vol. 110, 199–218, 2010.
12. Finkenzeller, K., *RFID Handbook: Fundamentals and Applications in contactless smart cards and Identifcation*, John Wiley & Sons, Inc., Publications, 2003.
13. Hagerty, J., F. Helmbrecht, W. McCalpin, R. Zane, and Z. Popovic, "Recycling ambient microwave energy with broadband rectenna arrays," *IEEE Transaction on Microwave Theory and Techniques*, Vol. 52, No. 3, 1014–1024, Mar. 2004.
14. Costanzo, A., A. Romani, D. Masotti, N. Abizzani, and V. Rizzoli, "RF/baseband co-design of switching receivers for multiband microwave energy harvesting," *Sensors and Actuators A: Physical*, Vol. 179, 158–168, Jun. 2012.
15. Cantatore, E., T. Geuns, G. Gelinck, E. Veenendaal, A. Gruijthuijsen, L. Schrijnemakers, S. Drews, and D. de Leeuw, "A 13.56 MHz RFID system based on organic transponders," *IEEE Journal of Solid State Circuits*, Vol. 42, No. 1, 84–92, Jan. 2007.
16. Subramanian, V., J. Frechet, P. Chang, D. Huang, J. Lee, S. Molesa, A. Murphy, D. Redinger, and S. Volkman, "Progress

toward development of all-printed rfid tags: Materials, processes, and devices," *Proceedings of the IEEE*, Vol. 93, No. 7, 1330–1338, Jul. 2005.

17. Steudel, S., K. Myny, V. Arkhipov, C. Deibel, S. D. Vusser, J. Genoe, and P. Heremans, "50 MHz rectifier based on an organic diode," *Nature Materials*, Vol. 4, 597–600, Aug. 2005.
18. Fortunato, E., N. Correia, P. Barquinha, L. Pereira, G. Goncalves, and R. Martins, "High-performance flexible hybrid field-effect transistors based on cellulose fiber paper," *IEEE Electron Device Letters*, Vol. 29, No. 9, 988–990, Sep. 2008.
19. Sekitani, T., Y. Noguchi, U. Zschieschang, H. Klauk, and T. Someya, "Organic transistors manufactured using inkjet technology with subfemtoliter accuracy," *Proceedings of the National Academy of Sciences of the USA*, Vol. 105, No. 13, 4976–4980, Apr. 2008.
20. Cardinali, M., L. Valentini, J. Kenny, and I. Mutlay, "Graphene based composites prepared through exfoliation of graphite platelets in methyl methacrylate/poly (methyl methacrylate)," *Polymer International*, Vol. 61, No. 7, 1079–1083, Jul. 2012.
21. Cosseddu, P., S. Lai, M. Barbaro, and A. Bonfiglio, "Ultra-low voltage, organic thin film transistors fabricated on plastic substrates by a highly reproducible process," *Applied Physics Letters*, Vol. 100, No. 9, 093305–093305-5, Feb. 2012.
22. Yang, L., A. Rida, R. Vyas, and M. Tentzeris, "RFID tag and RF structures on a paper substrate using inkjet-printing technology," *IEEE Transaction on Microwave Theory and Techniques*, Vol. 55, No. 12, 2894–2901, Dec. 2007.
23. Yang, L., L. J. Martin, D. Staiculescu, C. P. Wong, and M. Tentzeris, "Conformal magnetic composite RFID for wearable RF and bio-monitoring applications," *IEEE Transaction on Microwave Theory and Techniques*, Vol. 56, No. 12, 3223–3230, Dec. 2008.
24. Lakafosis, V., A. Rida, R. Vyas, L. Yang, S. Nikolaou, and M. Tentzeris, "Towards the first wireless sensor networks consisting of inkjet-printed, paper-based RFID-enabled sensor tags," *Proceedings of the IEEE*, Vol. 98, No. 9, 1601–1609, Sep. 2010.
25. Orecchini,G., V. Palazzari, A. Rida, F. Alimenti, M. Tentzeris, and L. Roselli, "Design and fabrication of ultra-low cost radio frequency identification antennas and tags exploiting paper substrates and inkjet printing technology," *IET Microwave Antennas & Propagation*, Vol. 5, No. 8, 993–1001, Jun. 2011.

26. Nelo, M., A. Sowpati, V. K. Palukuru, J. Juuti, and H. Jantunen, "Utilization of screen printed low curing temperature cobalt nanoparticle ink for miniaturization of patch antennas," *Progress In Electromagnetics Research*, Vol. 127, 427–444, 2012.
27. Basirico, L., P. Cosseddu, A. Scida, B. Fraboni, G. Malliaras, and A. Bonfiglio, "Electrical characteristics of ink-jet printed, all-polymer electrochemical transistors," *Organic Electronics*, Vol. 13, No. 2, 244–248, Feb. 2012.
28. Jingtian, X., Y. Na, C. Wenyi, X. Conghui, W. Xiao, Y. Yuqing, J. Hongyan, and M. Hao, "Low-cost low-power UHF RFID tag with on-chip antenna," *Journal of Semiconductors*, Vol. 30, No. 7, 075012/1–075012/6, Jul. 2009.
29. Law, M., A. Bermak, and H. Luong, "A sub-μW embedded CMOS temperature sensor for RFID food monitoring application," *IEEE Journal of Solid-State Circuits*, Vol. 45, No. 6, 1246–1255, Jun. 2010.
30. Snyder, E. J., *Alien Technology Corporation White Paper: Fluidic Self Assembly*, Alien Technology, 1999, [Online], Available: http://www.alientechnology.com.
31. Alimenti, F., M. Virili, G. Orecchini, P. Mezzanotte, V. Palazzari, M. Tentzeris, and L. Roselli, "A new contactless assembly method for paper substrate antennas and UHF RFID chips," *IEEE Transaction on Microwave Theory and Techniques*, Vol. 59, No. 3, 627–637, Mar. 2011.
32. Hertleer, C., H. Rogier, L. Vallozzi, and L. V. Langenhove, "A textile antenna for off-body communication integrated into protective clothing for firefighters," *IEEE Trans. on Antennas and Propagation*, Vol. 57, No. 4, 919–925, Apr. 2009.
33. Li, X., J. Liao, Y. Yuan, and D. Yu, "Eye-shaped segmented reader antenna for near-field UHF RFID applications," *Progress In Electromagnetics Research*, Vol. 114, 481–493, 2011.
34. Tiang, J.-J., M. T. Islam, N. Misran, and J. S. Mandeep, "Circular microstrip slot antenna for dual-frequency RFID application," *Progress In Electromagnetics Research*, Vol. 120, 499–512, 2011.
35. Amin, Y., Q. Chen, H. Tenhunen, and L.-R. Zheng, "Performance-optimized quadrate bowtie RFID antennas for cost-effective and eco-friendly industrial applications," *Progress In Electromagnetics Research*, Vol. 126, 49–64, 2012.
36. Amin, Y., Q. Chen, L.-R. Zheng, and H. Tenhunen, "Development and analysis of flexible UHF RFID antennas for "green" electronics," *Progress In Electromagnetics Research*, Vol. 130, 1–15, 2012.

37. Viani, F., M. Salucci, F. Robol, G. Olivieri, and A. Massa, "Design of UHF RFID/GPS fractal antenna for logistic management," *Journal of Electromagnetic Waves and Applications*, Vol. 26, No. 4, 480–492, 2012.
38. Springer, A., R. Weigel, A. Pohl, and F. Seifert, "Wireless identification and sensing using surface acoustic wave devices," *Mechatronics*, Vol. 9, No. 7, 745–756, Oct. 1999.
39. Chang, K., Y. Kim, Y. Kim, and Y. Yoon, "Functional antenna integrated with relative humidity sensor using synthesised polyimide for passive rfid sensing," *Electronic Letters*, Vol. 43, No. 5, 1918–1923, May 2007.
40. Shrestha, S., M. Balachandran, M. Agarwal, V. Phoha, and K. Varahramyan, "A chipless RFID sensor system for cyber centric monitoring applications," *IEEE Transaction on Microwave Theory and Techniques*, Vol. 57, No. 5, 1303–1309, May 2009.
41. Occhiuzzi, C., S. Cippitelli, and G. Marrocco, "Modeling, design and experimentation of wearable RFID sensor tag," *IEEE Trans. on Antennas and Propagation*, Vol. 58, No. 8, 2490–2498, Aug. 2010.
42. Ramos, A., A. Lazaro, D. Girbau, and R. Villarino, "Time-domain measurement of time-coded UWB chipless RFID tags," *Progress In Electromagnetics Research*, Vol. 116, 313–331, 2011.
43. Nair, R., E. Perret, and S. Tedjini, "Temporal multi-frequency encoding technique for chipless RFID applications," *IEEE MTT-S International Microwave Symposium Digest*, 1–3, Montreal, QC, Canada, Jun. 2012.
44. Potyrailo, R., C. Surman, S. Go, Y. Lee, T. Sivavec, and W. Morris, "Development of radio-frequency identification sensors based on organic electronic sensing materials for selective detection of toxic vapors," *Journal of Applied Physics*, Vol. 106, No. 12, 124902–124902-6, Dec. 2009.
45. Viikari, V. and H. Seppa, "RFID MEMS sensor concept based on intermodulation distortion," *IEEE Sensor Journal*, Vol. 9, No. 12, 1918–1923, Dec. 2009.
46. Riley, J., A. Smith, D. Reynolds, A. Edwards, J. Osborne, I. Williams, N. Carreck, and G. Poppy, "Tracking bees with harmonic radar," *Nature*, Vol. 379, 29–30, Jan. 1996.
47. Helbing, S., M. Cryan, F. Alimenti, P. Mezzanotte, L. Roselli, and R. Sorrentino, "Design and verification of a novel crossed dipole structure for quasi-optical frequency doublers," *IEEE Microwave and Guided Wave Letters*, Vol. 10, No. 3, 105–107, Mar. 2000.

48. Orecchini, G., L. Yang, A. Rida, F. Alimenti, M. Tentzeris, and L. Roselli, "Green technologies and RFID: Present and future," *Applied Comput. Electromagnetics Society Journal*, Vol. 25, No. 3, 230–238, Mar. 2010.
49. Steudel, S., S. D. Vusser, K. Myny, M. Lenes, J. Genoe, and P. Heremans, "Comparison of organic diode structures regarding high-frequency rectification behavior in radio-frequency identification tags," *Journal of Applied Physics*, Vol. 99, No. 11, 114519, Jun. 2006.
50. Valentini, L. and J. Kenny, "Novel approaches to developing carbon nanotube based polymer composites: Fundamental studies and nanotech applications," *Polymer*, Vol. 46, No. 17, 6715–6718, Aug. 2005.
51. Marinov, V., Y. Atanasov, A. Khan, D. Vaselaar, A. Halvorsen, D. Schulz, and D. Chrisey, "Direct-write vapor sensors on FR4 plastic substrates," *IEEE Sensor Journal*, Vol. 7, No. 6, 937–944, Jun. 2007.
52. Unander, T. and H.-E. Nilsson, "Characterization of printed moisture sensors in packaging surveillance applications," *IEEE Sensor Journal*, Vol. 9, No. 8, 922–928, Aug. 2009.
53. Couderc, S., B. Kim, and T. Someya, "Cellulose-based composite as a raw material for flexible ans ultra-lightweight mechanical switch devices," *IEEE 22nd International Conference on Micro Electro Mechanical Systems*, 646–649, Sorrento, Italy, Jan. 2009.
54. Bozzi, M., A. Georgiadis, and K. Wu, "Review of substrate-integrated waveguide circuits and antennas," *IET Microwave, Antennas & Propagation*, Vol. 5, No. 8, 909–920, Jun. 2011.
55. Alimenti, F., P. Mezzanotte, L. Roselli, and R. Sorrentino, "A revised formulation of modal absorbing and matched modal source boundary conditions for the efficient FDTD analysis of waveguide structures," *IEEE Transaction on Microwave Theory and Techniques*, Vol. 48, No. 1, 50–59, Jan. 2000.
56. Alimenti, F., P. Mezzanotte, G. Tasselli, A. Battistini, V. Palazzari, and L. Roselli, "Development of low-cost 24-GHz circuits exploiting system-in-package (SiP) approach on commercial PCB technology," *IEEE Trans. on Components, Packaging and Manufacturing Technology*, Vol. 2, No. 8, 1265–1274, Aug. 2012.
57. Lovei, G., I. Stringer, C. Devine, and M. Cartellieri, "Harmonic radar — A method using inexpensive tags to study invertebrate movement on land," *New Zealand Journal of Ecology*, Vol. 21, No. 2, 187–193, 1997.

58. Colpitts, B. and G. Boiteau, "Harmonic radar transceiver design: Miniature miniature tags for insect tracking," *IEEE Trans. on Antennas and Propagation*, Vol. 52, No. 11, 2825–2832, Nov. 2004.
59. Tu, W.-H., M.-Y. Li, and K. Chang, "Broadband microstrip-coplanar stripline-fed circularly polarized spiral antenna," *IEEE International Antennas and Propagation Symposium Digest*, Albuquerque (USA), 3669–3672, Oct. 2006.
60. Maas, S., *Nonlinear Microwave and RF Circuits*, 2nd Edition, Artech-House, Inc., 2003.
61. Monti, G., R. de Paolis, and L. Tarricone, "Design of a 3-state reconfigurable CRLH transmission line based on MEMS switches," *Progress In Electromagnetics Research*, Vol. 95, 283–297, 2009.
62. Lyu, J.-J. and T.-L. Chen, "Optimize a RFID-based turbine maintenance model - a preliminary study," *IEEE International Conference on Industrial Engineering and Engineering Management*, 501–505, Singapore, Nov. 2008.
63. Collin, R., *Antennas and Radiowave Propagation*, McGraw-Hill, 1985.